ORIGINAL RESEARCH

Turkish Journal of Immunology, 13(1):22-32

Impact of Genetic Background and Gender on Mouse Susceptibility to H1N1- PR8: Implication of the Host Immune Responses

Dina Nadeem Abd-Elshafy[1,3], Mohamed Hassan Nasraa[2,3], Rola Nadeem[2,3], Mahmoud Mohamed Bahgat[2,3,4]

[1]*The National Research Centre, Institute of Environmental Research and Climate Changes, Department of Water Pollution Research, Environmental Virology Laboratory, Cairo, Egypt;* [2]*The National Research Centre, Institute of Pharmaceutical and Drug Industries Research, Department of Therapeutic Chemistry, Cairo, Egypt;* [3]*The National Research Centre, the Center of Excellence for Advanced Sciences, Research Group Immune- and Bio-markers for Infection, Cairo, Egypt;* [4]*Egypt Center for Research and Regenerative Medicine, Cairo, Egypt*

Abstract

Objective: This study aimed to compare the susceptibility of different mouse strains to H1N1-PR8 influenza A virus (IAV) infection.

Materials and Methods: The virus was produced in 293T/ Madin-Darby canine kidney (MDCK) cells following a plasmid rescue protocol and then used to infect males of BALB/c, CD1 IGS (CD-1 imprinting control strain), and National Institutes of Health (NIH) Swiss mouse strain as well as both genders of C57BL/6J mice. Both serum virus-specific immunoglobulin M / immunoglobulin G (IgM/IgG) and interferon-gamma (IFN-ɣ) levels, as well as H1N1-RNA in lungs of infected mouse strains, were investigated.

Results: Differential body weight with superior loss was recorded in the C57BL/6J. Differential virus-IgM/IgG levels were recorded with higher IgM in the BALB/c (p=0.001) and higher IgG in the CD1 IGS (p=0.022). The C57BL/6 males were more susceptible to H1N1 infection and mounted higher IgM compared to females (p=0.001), whereas females showed higher IgG than males (p=0.034). Differential IFN-γ levels were observed among male mice of various strains, with a notable increase in BALB/c mice (p=0.071) and a significant decrease in C57BL/6J mice (p=0.035). A significant increase in the IFN-ɣ level was recorded in C57BL/6J females compared to males (p=0.015). The viral RNA was almost equal in the lungs of the males of various infected mouse strains' and in both genders of the infected C57BL/6J.

Conclusion: The studied host factors can be partially implicated in the recorded differential susceptibility of various mouse strains to infection with the H1N1-PR8 IAV. Our results can help in selecting the proper mouse model for vaccine evaluation and can be translated to future human studies to identify the highly susceptible individuals to influenza infection and learn more about the host factors involved in resistance to IAV infection.

Keywords: H1N1-PR8 influenza A virus, mice of different genetic backgrounds, IgM/IgG and IFN-ɣ levels

Correspondence
Mahmoud Mohamed Bahgat

E-mail
mbahgatriad@yahoo.com

Received
October 12, 2024

Accepted
February 14, 2025

Published
April 29, 2025

Suggested Citation
Abd-Elshafy DN, Nasraa MH, Nadeem R, Bahgat MM. Impact of genetic background and gender on mouse susceptibility to H1N1- PR8: Implication of the host immune responses. Turk J Immunol. 2025;13(1):22-32.

DOI
10.36519/tji.2025.565

Introduction

Due to feasibility, small size, easiness of handling and maintaining in an animal house, uncomplicated ethical approval to work with, and a high degree of homology to both the human genome and metabolome (1-3), the mouse has always been considered as a very suitable animal model to study virus pathogenesis and understand host susceptibility to virus infection.

Within a given mouse strain, individual animals do not respond similarly to infection (4-7). Also, strains of different genetic backgrounds behave differently in their response to infection (8, 9). Understanding the reasons behind intra- and inter-strain individualized responses might significantly contribute to our understanding of human personalized response to infection. Differential expression of proteases involved in function, cleavage, and activation of virus virulence molecules among mouse strains of different genetic backgrounds could differentially affect infection outcome (10), and their inhibition could block virus infection (11). Also, differential regulation of immune responses in mouse strains of different genetic backgrounds could differentially affect their susceptibility to virus infection (12).

In this study, we compared the susceptibility of BALB/c, C57BL/6J, CD1 IGS (CD-1 imprinting control strain) and National Institutes of Health (NIH) Swiss mouse strains to the H1N1-PR8 influenza A virus (IAV) infection. We also compared the anti-H1N1 immune responses of these mouse strains upon infection to learn how resistant/susceptible mouse strains serologically respond to IAV infection.

Materials and Methods

Production of the PR8-H1N1 Virus in Cell Culture

Constructs of the cloned 8 PR8-H1N1 genes in the pHW2000 vector, which encode for the virus hemagglutinin (HA), matrix (M), neuraminidase (NA), nucleoprotein (NP), nonstructural protein (NS), polymerase acidic protein (PA) and polymerase subunits (PB1 and PB2) as well as the empty plasmid, were kindly provided by Prof. Richard Webby at St. Jude Children Hospital, Memphis, the USA through a fully executed material transfer agreement (MTA) with Prof. Mahmoud Mohamed Bahgat. Plasmids encoding individual PR8-H1N1 segments were used to transfect competent *Escherichia coli* bacterial cells (Invitrogen; Thermo Fisher Scientific Inc., USA) in the presence of ampicillin, as the plasmid contains an ampicillin resistance gene. To prepare stocks of the constructs encoding the individual influenza virus proteins, the growing colonies carrying each construct were subjected to plasmid midi-preparations (Qiagen, Germany), and the concentrations of the purified plasmids were quantified using a NanoDrop 1000 spectrophotometer (Thermo Fisher Scientific Inc., USA). Both their purity and integrity were checked by electrophoresis on 1.1% agarose gel (Promega) followed by visualization using ethidium bromide (EtBr) staining solution, Sigma-Aldrich (Merck KGaA, Germany) in the presence of a molecular weight marker (Promega Corp., USA). The production of the PR8-H1N1 virus in cell culture was done through the plasmid rescue protocol as formerly described (13). Briefly, the equimolar ratio of the individual constructs encoding the PR8-H1N1 8 proteins was mixed and used to co-transfect 293T cells co-cultured with Madin-Darby canine kidney (MDCK) cells (both from the American Type Culture Collection - ATCC) and incubated at 37°C, 5% CO_2. Control wells where cells were transfected with empty plasmids were included. Cells were assessed daily for the development of cytopathic effect (CPE) in the MDCK sheet as a result of the virus propagation. Once the CPE became obvious, the medium containing the PR8-H1N1virus was harvested and centrifuged at 1200 g for 5 minutes. The supernatant was collected, divided into aliquots, and subjected to slow deep freezing overnight in Mr. Frosty™ Freezing Container (Thermo Fisher Scientific Inc., USA) (-80°C, cooled with isopropanol).

Titration of the Generated PR8-H1N1 Virus

The generated virus was propagated in MDCK, as previously reported by us and others (13, 14). Briefly, MDCK cells were co-incubated with the stock PR8-H1N1 virus diluted in infection medium (Dulbecco's modified eagle medium [DMEM]-GlutaMax; 1% penicillin/streptomycin, 1 mM sodium pyruvate, 1% bovine serum albumin, 2 µg/mL tosyl-phenylalanyl-chloromethyl ketone-treated trypsin [TPCK-trypsin]) (Invitrogen; Thermo Fisher Scientific Inc., USA) and with 10-fold dilutions (10-1 to 10-6) for one hour (h) at 37°C, 5% CO_2. The infection medium was discarded, wells were washed and then coated with agarose overlayer diluted 1:1 with 2X concentrated culture medium (DMEM) to a final concentration of 1%. Then, plates were returned to 37°C, 5% CO_2, and the formed plaques were monitored within the following 48-72 h. Control wells were included in the same plates;

they were treated with a virus-free infection medium and the agarose overlay to ensure that the observed CPE was because of the virus and not because of any stress caused while manipulating the MDCK cells. For visualization of the growing plaques, wells were first fixed for 1 h in 4% formaldehyde solution, Sigma-Aldrich (Merck KGaA, Germany), stained using 1% crystal violet Staining Solution, Sigma-Aldrich (Merck KGaA, Darmstadt, Germany) diluted in 10% ethanol/acetic acid mixture for 15 minutes, then destained with continuous water flow till appearance of white plaques in blue cells background.

Mice Infection

BALB/c, C57BL/6J, CD1 IGS, and NIH Swiss mice were bred and maintained at the animal house of the National Research Centre (NRC). Animals were fed on a standard diet and maintained at ambient temperature according to the animal welfare protocols of the NRC in Egypt. Anesthesia procedures complied with the guidelines of the National Institutes of Health in the USA and were approved by the Medical Ethical Committee of the NRC (MREC Registration number: 17-120). Mice infection was carried out according to our previous report (11). Of each strain, five animals received intranasal infection with H1N1-PR8 (2×10^3 plaque-forming units [PFU] in 25 µL/mouse) diluted in phosphate-buffered saline (PBS) and five animals received PBS (25 µL each) as a control group. Weight loss and survival of infected mice were followed over a period of 11 days. Animals were relaxed by being anesthetized with discontinuous sniffs of diethyl ether vapor before infection and before recording body weight. After 14 days, animals were fully anesthetized with the ketamine-xylazine mixture, Sigma-Aldrich (Merck KGaA, Germany), and blood samples were collected from individual mice by inserting a heparinized capillary tube into the orbital optical venous plexus. Sera were separated by centrifugation of individual blood samples at 10,000 g, divided into multiple aliquots, and frozen at –80°C until being used.

Detection of Virus-Specific Immunoglobulin M / Immunoglobulin G (IgM/IgG) in Sera from the Infected Mouse Strains

Quantification of the immunoglobulin classes in sera of infected and control groups of various mouse strains was performed according to our published protocol with minor modifications (15). Briefly, the ELISA plates were coated (100 µL/well) with killed H1N1-PR8 virus (10^6 PFUs/mL) diluted 1:1 in coating buffer (1 M Na_2CO_3; 1 M $NaHCO_3$, pH 9.6) and incubated at 37°C for 3 h. Plates were washed thrice with PBS–0.05% Tween 20 (PBST). None specific binding was blocked by incubating the plates with PBST–5% fetal bovine serum (PBST–FBS; 200 µL/well) at 37°C for 2 h. After washing thrice with PBST, wells were loaded with diluted mice sera in PBST–FBS (1:50; 100 µL/well), and plates were incubated at 37°C for 2 h. Plates were washed thrice and then incubated with 1:2000 (100 µL/well) anti-mice IgM/IgG conjugated to horseradish peroxidase (Kirkgaard & Perry Laboratories, Germany) at 37°C for 2 h, followed by washing plates thrice with PBST. For color development, 100 µL/well O-phenylenediamine (OPD) substrate Sigma-Aldrich (Merck KGaA, Germany) was diluted in substrate buffer (0.1 M anhydrous citric acid and 0.2 M dibasic sodium phosphate, pH 5.0) containing 0.06% H_2O_2, and plates were left for 10 minutes at room temperature until color developed. The enzymatic reaction was stopped with 40 µL/well 2 M HCl, and the changes in the optical density (OD) in plate wells were recorded at a λmax of 490 nm using a multi-well SUNRISE plate reader (TECAN Group LTD., Switzerland).

IFN-γ Detection in Sera from the Infected Mouse Strains

IFN-γ levels in sera of various infected mouse strains were measured using an indirect ELISA assay. The microtiter plates (SPL Life Sciences Co. Ltd., South Korea) were coated in duplicates with 50 µL of individual mouse sera diluted 1:25 in carbonate/bicarbonate coating buffer and incubated at 37°C overnight. Plate wells were blocked with 100 µL blocking buffer containing 5% fetal bovine serum (Serana Europe GmbH, Germany) in phosphate buffer saline-0.05% Tween-20 (LobaChemie PVT, LTD, India) for 1 h. Rat anti-mouse IFN-γ antibody (Biolegend, USA) was applied 50 µL of 1:1000 dilution (5 µg/mL) followed by 2 h incubation at 37°C. Horseradish peroxidase (HRP)-labeled anti-rat IgG antibody (KPL; USA) was applied 50 µL of 1:1000 dilution (5 µg/mL) and incubated for 1 h at 37°C. OPD substrate, Sigma-Aldrich (Merck KGaA, Germany), was used at 0.04% in citrate buffer supplemented with 30% H_2O_2, 50 µL was applied to each well and incubated for 10 minutes at 37°C, and the reaction was stopped using 50 µL 2M H_2SO_4. Absorbance was measured at 492 nm, and a reference wavelength at 620 nm filters (Clindiag Systems Co., Ltd., China).

Quantification of Viral RNA in the Lungs of Infected Mouse Strains

QIAamp viral RNA purification kit was used to extract the nucleic acid of the H1N1-PR8 virus from individual

lung tissues of various mouse strains. RNA concentrations were quantified using a NanoDrop 1000 spectrophotometer (Thermo Fisher Scientific Inc., USA). Specific forward (F) and reverse (R) primers were used to amplify the H1N1-PR8-HA segment by quantitative reverse transcription polymerase chain reaction RT-PCR (qRT-PCR) of the extracted RNA from individual mice (14). The R primer was initially used to reverse transcribe the virus RNA into cDNA using SuperScript III reverse transcriptase (Invitrogen; Thermo Fisher Scientific Inc., USA). The cDNA was quantified using the SYBR Green I Master kit (Roche, Switzerland) in a Rotor-Gene-Q 6000 real-time PCR cycler. The cycling conditions of the conventional PCR included initial denaturation at 94°C for 3 minutes followed by 40 amplification cycles each of denaturation at 94°C for 30 seconds, annealing at 48°C for 1 minute, and extension at 72°C for 1 minute. The program included a final extension at 72°C for 10 minutes.

Statistical Analysis

Statistical analysis and plots were done using the GraphPad PRISM version 5 software (GraphPad Software Inc., USA). Results were expressed as means ± standard deviations (SDs). Statistical significance was calculated by comparing the differences between the means of different studied groups using the Student's t-test. Differences were considered significant when the *p*-value was <0.05.

Results

The H1N1-PR8 Virus Rescue and Analysis of Its Infectivity

Visualizing midi preps of the eight plasmids encoding for influenza virus HA, M, NA, NP, NS, PA, PB1, and PB2 on agarose gel side by side with the empty pHW2000 vector and molecular weight marker revealed both their purity, integrity, and correct relative migration with respect to the molecular weights of the eight inserts. As demonstrated, the eight constructs showed slower migration (higher molecular weight) than the empty vector (EV) (Figure 1A).

Using the supernatant (medium) of co-transfected 293T/MDCK cells with the eight plasmids to infect MDCK cells in a plaque infectivity assay revealed high titer of the produced virus that caused complete damage of the cell monolayer until titer of 10^{-2}, the plaques became

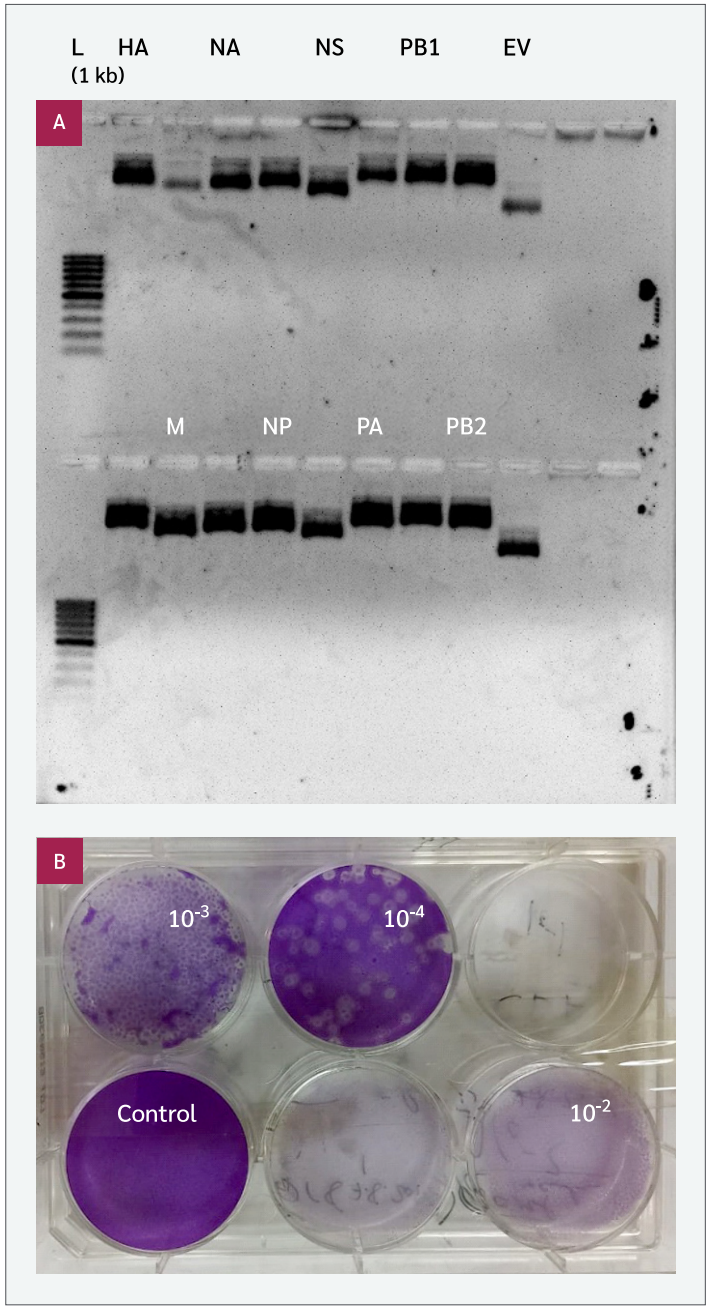

Figure 1. The H1N1-PR8 influenza A virus rescue and analysis of its infectivity. **(A)** Visualizing the midi preps of the eight plasmids encoding for the influenza HA, M, NA, NP, NS, PA, PB1 and PB2 on agarose gel side by side with the empty pHW2000 vector and molecular weight ladder (1kb). Both the purity and integrity of the eight inserts were indicated and the eight constructs showed slower migration than the empty vector. The ladder (L), HA, NA, NS, PB1 and EV bands are in the up section while the M, NP, PA and PB2 are in the down section of the gel. **(B)** Plaque infectivity assay for the produced virus. The medium of co-transfected 293T/MDCK cells with the 8 plasmids was used to infect MDCK cells. The results revealed high titer of the produced virus that caused complete damage of the cell monolayer until titer of 10^{-2}, the plaques became visible but uncountable at 10^{-3} and could be counted at 10^{-4}, whereas, the control cells remained intact.

visible but uncountable at 10^{-3} and could be counted at 10^{-4} whereas, the control uninfected cells layer remained totally intact (Figure 1B).

Susceptibility of the Various Mouse Strains' Males and Both Genders of the C57BL/6 to H1N1-PR8 Infection

The BALB/c, C57BL/6J, CD1 IGS, and NIH Swiss male mice showed differential susceptibilities to the produced H1N1-PR8 IAV as reflected by their differential body-weight loss at different days (d) post-infection (pi) with the top weight loss recorded for C57BL/6J males which reached its peak (25% loss) at d8 pi. In contrast, none of the control, PBS-given male mice of different strains, showed body weight loss (Figure 2A).

Since the C57BL/6J males showed the top body weight loss upon the H1N1-PR8 infection, we decided to compare their susceptibility on the gender level. Of interest, the results showed a gender-specific pattern as recorded by a sharp weight loss in female mice between d1-3 pi, which reached its peak at d3 pi (~20% loss), followed by regaining weight that never reached the starting weight (stayed at 10% loss), whereas, male mice continued to lose weight to reach its peak (25% loss) at d8 pi followed by slight regaining weight thereafter (Figure 2B).

Serum Levels of Virus-Specific IgM/IgG in Various Mouse Strains' Males and Both Genders of the C57BL/6 Post Infection

The IgM levels were significantly higher in the BALB/c, CD1 IGS, C57BL/6J, and NIH mouse strains' males compared to control ones (p=0.001, p=0.011, p=0.016, and p=0.007, respectively) (Figure 3A). In comparison, only the infected males of the CD1 IGS and NIH strains showed a significant increase in IgG levels than the PBS-given ones (p<0.05) (Figure 3B).

Generally, serum IgM and IgG levels were significantly higher in the C57BL/6J infected mice (p=0.0003 and p=0.0025, respectively, for females; p=0.0002 and p=0.0014, respectively, for males) compared to the control mice with a significantly higher IgM level recorded for the infected males (p=0.001) (Figure 4A), and IgG level for the infected females (p=0.034) (Figure 4B).

Interferon-gamma (IFN-ɣ) Levels in Various Mouse Strains' Males and Both Genders of the C57BL/6J Post Infection

Obvious strain-specific variations in the IFN-γ levels were observed, where both the CD-1IGS and C57BL/6J mouse strain males showed non-significant (p=0.142) and significant (p=0.035) decreases in the IFN-ɣ levels

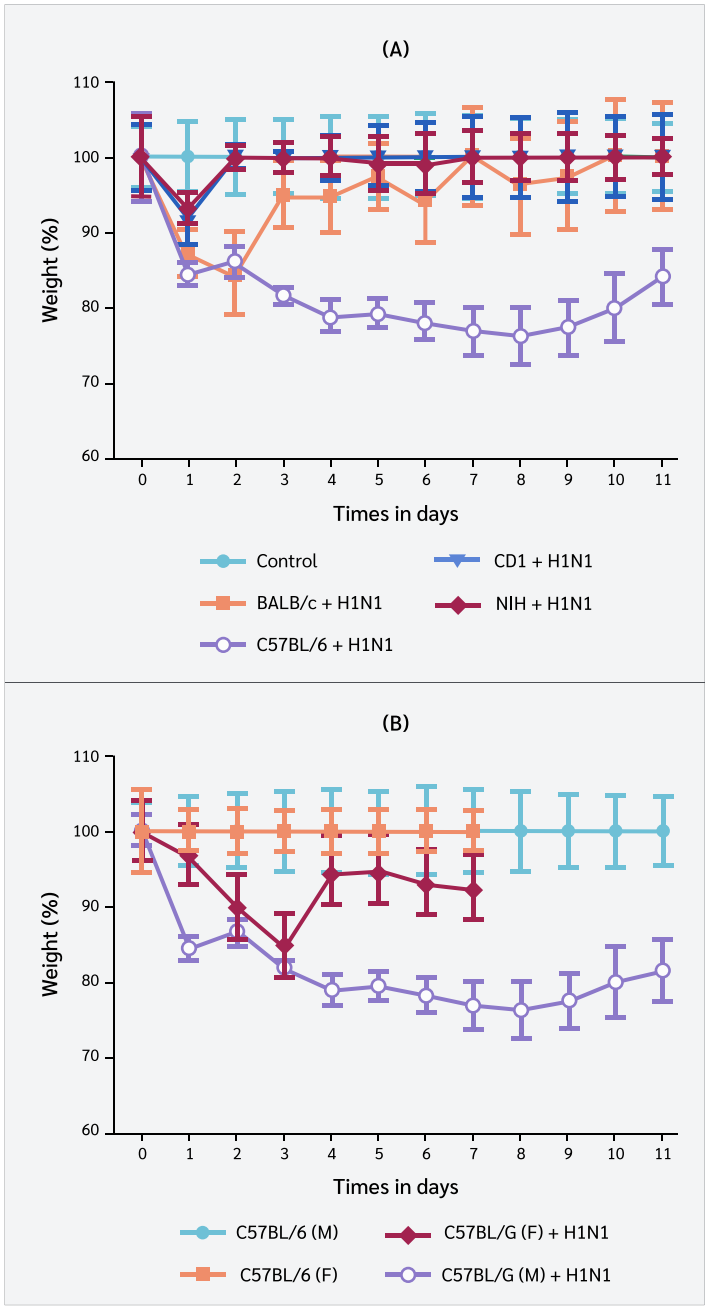

Figure 2. Susceptibility of the mouse strains' males **(A)** and C57BL/6J both genders **(B)** to the H1N1-PR8 infection. The BALB/c, C57BL/6J, CD1 IGS and NIH Swiss male mice (n=5 each) were either intranasally infected with diluted H1N1-PR8 in PBS (2 × 10^3 plaque forming units (PFU) in 25 µL/ mouse) or received PBS (25 µL each) as control group. Weight loss and survival of infected mice was followed over a period of 14 days. Animals were relaxed by being anesthetized with discontinuous sniffs of diethyl ether vapor before infection and before recording bodyweight.

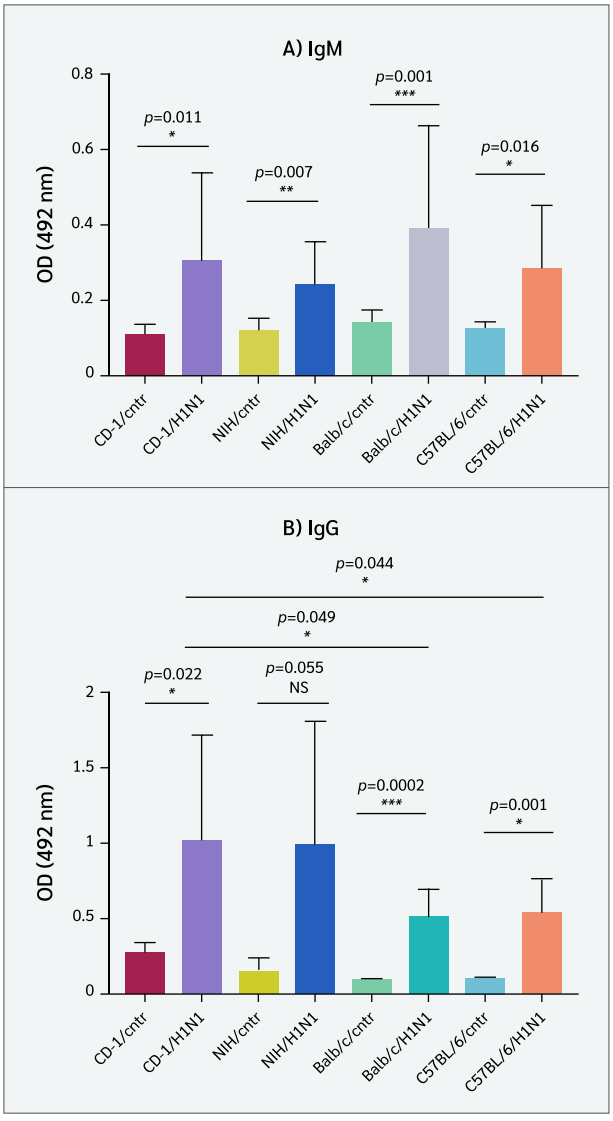

Figure 3. Serum levels of virus-specific IgM (A) and IgG (B) in the mouse strains' males post infection. IgM and IgG levels in the infected and control males (n=5 each) from various mouse strains were measured using ELISA.

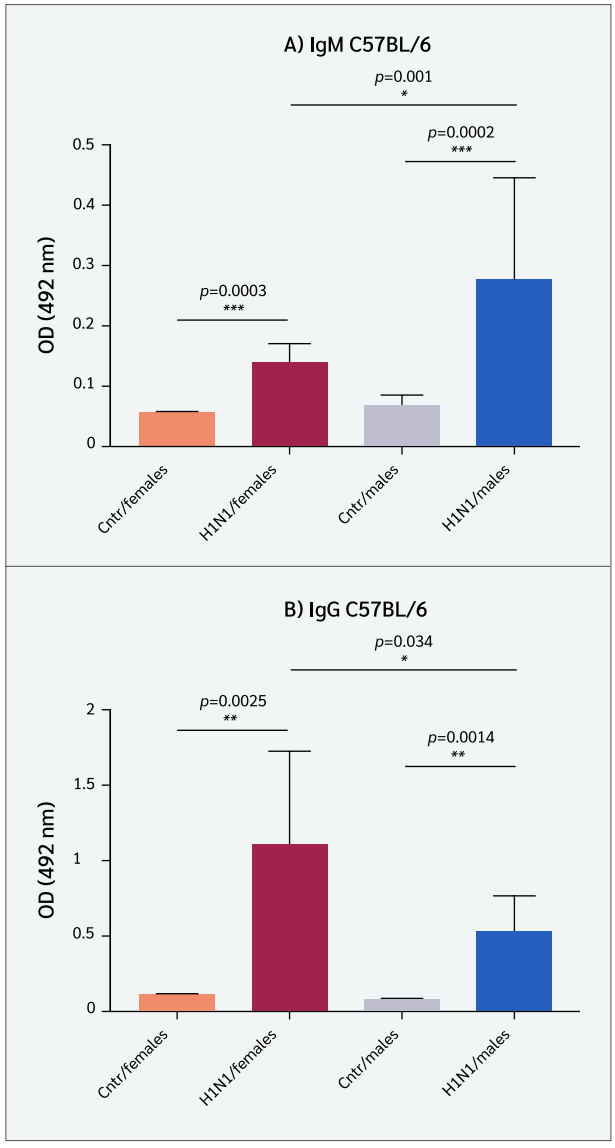

Figure 4. Serum levels of virus-specific IgM (A) and IgG (B) in the C57BL/6J both genders post infection. IgM and IgG levels in the infected and control mice from both genders (n=5 each) were measured using ELISA.

compared to control mice. Both the NIH and BALB/c mouse strains' males showed non-significant increases in the IFN-ɣ levels (p=0.571 and p=0.071, respectively) compared to control mice (Figure 5A).

Gender-specific IFN-ɣ levels were noticed in the C57BL/6J mouse strain, where IFN-ɣ level was significantly higher in the infected females (p=0.0337) compared to control ones. A non-significant decrease in the IFN-ɣ level was recorded in infected males (p=0.111) compared to control mice (Figure 5B).

The IFN-ɣ means in the PBS-received and H1N1-PR8 infected mouse strain males were 1.203667 and 0.7261, respectively, for the CD1 IGS; 0.6645 and 0.7908, respectively, for the NIH; 0.811667 and 1.1907, respectively, for BALB/c. The gender levels of the C57BL/6J means were 1.3515 and 0.9433, respectively, for females, whereas they were 1.0556 and 1.292125, respectively, for males.

Finally, the IFN-ɣ fold change in the infected mouse strains was 0.60323993 for the CD1 IGS males,

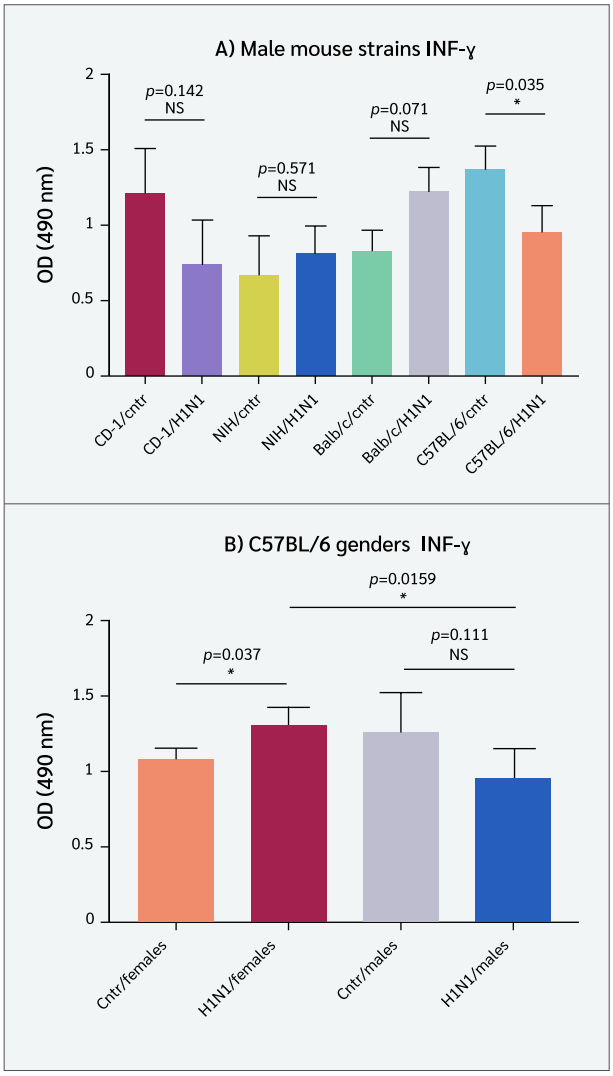

Figure 5. Interferon gamma (IFN-γ) levels in the mouse strains' males (A) and C57BL/6J both genders (B) post infection. IFN-γ levels in the infected and control mice (n=5 each) from all groups were measured using ELISA.

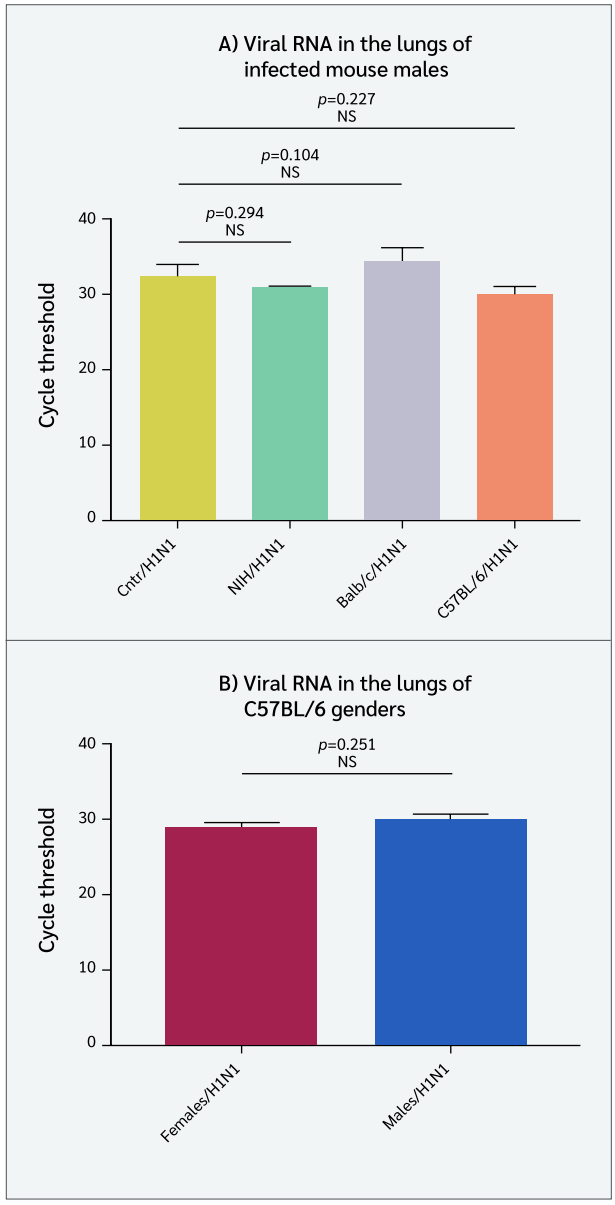

Figure 6. Viral RNA detection in the lungs of mouse strains' males (A) and the C57BL/6J both genders. (B) post infection. The virus RNA was extracted, The H1N1-PR8 HA was initially transcribed by specific R primer into cDNA using SuperScript III reverse transcriptase. The cycle threshold (Ct) means corresponding to HA virus RNA in the lungs of infected mouse strains and C57BL/6J genders was quantified by quantitative RT-PCR (qRT-PCR) using HA specific forward (F) and reverse (R) primers and the SYBR Green I Master kit in a Rotor-Gene-Q 6000 real-time PCR cycler.

1.19006772 for the NIH males, 1.46698092 for the BALB/c males, 0.69796522 for the C57BL/6J females, and 1.22406688 for the C57BL/6J males compared to the control mice of the same strain and gender.

Viral RNA Detection in the Lungs of Mouse Strains' Males and Both Genders of the C57BL/6 Post H1N1 Infection

Although not high, slight differences in the viral RNA levels were recorded in the lungs of infected mouse strains, as revealed by the cycle threshold (Ct) values. The lowest mean Ct values, i.e., the highest virus RNA levels, were recorded in the lungs of C57BL/6J males (p=0.227), NIH Swiss males (p=0.294), followed by BALB/c males (p=0.104) (Figure 6A). On gender levels, the mean viral RNA Ct value was slightly higher in the C57BL/6J males than in females (p=0.251) (Figure 6B).

Discussion

The high titer plaque count of the H1N1-PR8 we produced by the plasmid rescue protocol confirms the infectivity of the generated virus and the validity of the early reported protocol to generate influenza viruses by transfecting mammalian cells with plasmids encoding for the eight IAV proteins (13).

The differential body weight loss and susceptibility of various mouse strains to infection with the generated H1N1-PR8 virus agrees with previous reports on influenza and SARS-CoV2, though using different mouse strains, and may be attributed to differential expression of proteases involved both in the activation and functional cleavage of influenza HA which is mandatory for infecting host cells (8, 9-11). Also, the differential body weight loss of the studied mouse strains upon infection with the H1N1-PR8 can be referred to the previously reported differential regulation of immune responses in mouse strains of various genetic backgrounds, which can differentially influence their susceptibility to infection (12). This finding agrees with the differential anti-H1N1-IgM/IgG levels observed in the mouse strains studied in our study; post-H1N1 infection with the highest IgM levels seen in the BALB/c and the CD1 IGS mice and the highest IgG levels recorded in the CD1 IGS and NIH Swiss mice, which all did not show obvious weight loss upon infection.

BALB/c and C57BL/6J are inbred mouse strains that exhibit Th2- and Th1-biased immune responses, respectively, with C57BL/6J mice known for their higher susceptibility to diet-induced obesity. However, CD1 IGS and NIH Swiss are outbred mouse strains with genetic diversity favoring robust immune responses or displaying high reproductive performance and general adaptability, respectively (16).

Mouse genetic background can greatly impact the immune responses to virus infection (17). Research has demonstrated that BALB/c and C57BL/6J strains have different immune profiles, where BALB/c shows a Th2-biased response, which is linked to increased antibody production, while C57BL/6J mounts a Th1-biased response, which is marked by an increased pro-inflammatory cytokine production (18, 19). These variances might be among the factors leading to variations in the susceptibility and the course of the disease after IAV infection.

Studies comparing the pathogenicity of avian influenza A/H7N9 virus infection in these strains revealed that both showed significant weight loss and lung damage; however, the underlying immune mechanisms varied, indicating that the genetic background is a key factor in regulating the immune responses to influenza viruses (20, 21). On the other hand, we could not find reports concerning infection of the CD1 IGS and NIH Swiss strains with the H1N1-PR8 IAV, but it is known that outbred strains like both have more genetic variability than inbred strains.

The differential mouse gender susceptibility we saw in the present study was reported by others previously, showing that male C57BL/6J mice are more susceptible than females. Specific variants in the Y chromosome were shown to increase susceptibility to IAV infection in males and augment pathogenic immune responses in the lung, including activation of pro-inflammatory IL-17-producing γδ T cells, without affecting viral replication (22-25).

Of note, we found that the anti-H1N1-IgM levels were higher among C57BL/6J males than females, while the anti-H1N1-IgG levels were higher among females than males. This finding might indicate that IgG, but not IgM, is the essential immunoglobulin class in neutralizing the IAV infection. The observed heterogeneity in the levels of IFN-ɣ in control, PBS-given, studied mouse strains reflects the influence of genetic background on the regulation of IFN-ɣ production and could support our suggestion of a differential susceptibility of those mouse strains to H1N1 infection as evidenced by both differential bodyweight loss and differential antibody responses to infection.

In agreement with our results, several studies reported a clear impact of genetic backgrounds on IFN-γ production in different mouse strains (26, 27). The noticed drop in the IFN-γ levels in the infected C57BL/6J mice compared to the PBS-given mice is directly proportional to the drop in the body weight of the same mouse strain upon infection. It points out the partial implication of this cytokine in host susceptibility to influenza infection. Consistent with our findings, several studies proved that H1N1 infection can decrease IFN-γ levels in mice, contributing to impaired viral clearance, increased disease severity, and enhanced susceptibility to secondary bacterial infections (26, 28, 29). Unlikely, H1N1 infection induced an increase in the IFN-ɣ levels in the BALB/c

and NIH mice compared to control animals, and this might be partially the reason why these mouse strains did not lose weight upon infection. In agreement with our results, several studies demonstrated that infection of mice with H1N1 induces an increase in IFN-ɣ levels, which is associated with enhanced antiviral immune responses and improved outcomes (26, 30, 31).

The only conflicting result is that although infection caused a drop in the IFN-γ levels in CD1 IGS mice, they did not lose weight upon infection, yet, from our particular point of view, this reflects the complexity of the genetic susceptibility of mouse strains to infection which extends beyond interferon regulation and involves many other players. At the gender level, the recorded recovery of the body weight loss in the female C57BL/6J mice between days 3-4 coincides with the observed increase of the IFN-γ upon infection of this animal group. Similar results have been previously reported where female mice exhibited higher production of IFN-ɣ level compared to male mice, suggesting that gender influences the immune response to H1N1 infection (32).

In another study, ovariectomized female mice, which lack ovarian hormones such as estrogen, exhibited reduced IFN-ɣ production compared to intact females. This suggests that sex hormones, particularly estrogen, may contribute to the gender differences observed in IFN-γ response to H1N1 infection (33). Contrarily, infection of the C57BL/6J male mice resulted in a drop in the IFN-ɣ levels, which might explain why male mice did not regain body weight until day 11.

In contrast to our findings and on the innate immunity level, another report showed that male mice exhibited higher levels of pro-inflammatory cytokines, including IFN-ɣ, compared to female mice, which suggests gender-related differences in the immune responses corresponding to variations in the innate immune activation (34). While these studies provide evidence for gender-related differences in IFN-ɣ response to H1N1 infection in mice, further research is needed to fully understand the underlying mechanisms and whether similar findings can be extrapolated to humans. Finally, the recorded latest Ct values in the qRT-PCR detection of the virus RNA in lungs of BALB/c, CD1 IGS, NIH Swiss, and the earliest among the C57BL/6J illustrate the differential influenza infectivity of the mice from different genetic backgrounds.

Study Limitations

First, the sample size of animals per group in the study is relatively low. Second, the live virus in the lungs of infected mouse strains was not titrated by plaque infectivity assay. Therefore, we plan to design a larger-scale study with adequate mice numbers per group and include the missing assays.

Conclusion

The studied host factors can be partially behind the recorded differential susceptibility of various mouse strains to infection with the H1N1-PR8 IAV. Our findings can help in selecting the proper mouse model for evaluating anti-IAV-vaccines. They can also be translated to future human studies to identify the highly susceptible individuals to influenza infection and learn more about the host factors involved in resistance to IAV infection.

Ethics Committee Approval: Animals' maintenance, manipulation and applied anaesthesia procedures are complied with the guidelines of the National Institutes of Health in the USA and are approved by the Medical Ethical Committee of the NRC (MREC Registration number: 17-120).

Informed Consent: N.A.

Peer-review: Externally peer-reviewed

Author Contributions: Concept – M.M.B.; Design – M.M.B., D.N.A.; Supervision – D.N.A.; Fundings – M.M.B.; Materials – D.N.A., R.N., M.H.N.; Data Collection and/or Processing – D.N.A., M.H.N., R.N.; Analysis and/or Interpretation – D.N.A., M.H.N., R.N.; Literature Review – M.H.N., R.N.; Writer – M.M.B., M.H.N.; Critical Reviews – M.M.B.

Conflict of Interest: The authors declare no conflict of interest.

Financial Disclosure: This study was funded by grant 12060115 from the National Research Centre of Egypt, awarded to Mahmoud Mohamed Bahgat.

Acknowledgements: We acknowledge Prof. Richard Webby from the Department of Infectious Diseases, St. Jude Children's Research Hospital, Memphis, Tennessee, for providing the plasmids used to generate the H1N1-PR8 virus by reverse genetics.

References

1 Fuchs H, Gailus-Durner V, Adler T, Pimentel JA, Becker L, Bolle I, et al. The German Mouse Clinic: a platform for systemic phenotype analysis of mouse models. Curr Pharm Biotechnol. 2009;10(2):236-43. [CrossRef]

2 Du Y, Zhang W, Qiu H, Xiao C, Shi J, Reid LM, et al. Mouse models of liver parenchyma injuries and regeneration. Front Cell Dev Biol. 2022;10:903740. [CrossRef]

3 Pap A, Cuaranta-Monroy I, Peloquin M, Nagy L. Is the mouse a good model of human PPARγ-related metabolic diseases? Int J Mol Sci. 2016;17(8):1236. [CrossRef]

4 Bharucha T, Cleary B, Farmiloe A, Sutton E, Hayati H, Kirkwood P, et al. Mouse models of Japanese encephalitis virus infection: A systematic review and meta-analysis using a meta-regression approach. PLoS Negl Trop Dis. 2022;16(2):e0010116. [CrossRef]

5 Kamiya T, Greischar MA, Schneider DS, Mideo N. Uncovering drivers of dose-dependence and individual variation in malaria infection outcomes. PLoS Comput Biol. 2020;16(10):e1008211. [CrossRef]

6 Osbelt L, Thiemann S, Smit N, Lesker TR, Schröter M, Gálvez EJC, et al. Variations in microbiota composition of laboratory mice influence *Citrobacter rodentium* infection via variable short-chain fatty acid production. PLoS Pathog. 2020;16(3):e1008448. [CrossRef]

7 Contreras C, Newby JM, Hillen T. Personalized virus load curves for acute viral infections. Viruses. 2021;13(9):1815. [CrossRef]

8 Li K, Shen Y, Miller MA, Stabenow J, Williams RW, Lu L. Differing susceptibility of C57BL/6J and DBA/2J mice-parents of the murine BXD family, to severe acute respiratory syndrome coronavirus infection. Cell Biosci. 2021;11(1):137. [CrossRef]

9 Srivastava B, Błazejewska P, Hessmann M, Bruder D, Geffers R, Mauel S, et al. Host genetic background strongly influences the response to influenza a virus infections. PLoS One. 2009;4(3):e4857. [CrossRef]

10 Blazejewska P, Koscinski L, Viegas N, Anhlan D, Ludwig S, Schughart K. Pathogenicity of different PR8 influenza A virus variants in mice is determined by both viral and host factors. Virology. 2011;412(1):36-45. Erratum in: Virology. 2014;450-451:369-70. [CrossRef]

11 Bahgat MM, Błazejewska P, Schughart K. Inhibition of lung serine proteases in mice: a potentially new approach to control influenza infection. Virol J. 2011;8:27. [CrossRef]

12 Alberts R, Srivastava B, Wu H, Viegas N, Geffers R, Klawonn F, et al. Gene expression changes in the host response between resistant and susceptible inbred mouse strains after influenza A infection. Microbes Infect. 2010;12(4):309-18. [CrossRef]

13 Hoffmann E, Neumann G, Kawaoka Y, Hobom G, Webster RG. A DNA transfection system for generation of influenza A virus from eight plasmids. Proc Natl Acad Sci U S A. 2000;97(11):6108-13. [CrossRef]

14 Reina J, Fernandez-Baca V, Blanco I, Munar M. Comparison of Madin-Darby canine kidney cells (MDCK) with a green monkey continuous cell line (Vero) and human lung embryonated cells (MRC-5) in the isolation of influenza A virus from nasopharyngeal aspirates by shell vial culture. J Clin Microbiol. 1997;35(7):1900-1. [CrossRef]

15 Bahgat MM, Kutkat MA, Nasraa MH, Mostafa A, Webby R, Bahgat IM, et al. Characterization of an avian influenza virus H5N1 Egyptian isolate. J Virol Methods. 2009;159(2):244-50. [CrossRef]

16 Bryda EC. The Mighty Mouse: the impact of rodents on advances in biomedical research. Mo Med. 2013;110(3):207-11.

17 Zhao G, Liu C, Kou Z, Gao T, Pan T, Wu X, et al. Differences in the pathogenicity and inflammatory responses induced by avian influenza A/H7N9 virus infection in BALB/c and C57BL/6 mouse models. PLoS One. 2014;9(3):e92987. [CrossRef]

18 Rottmann BG, Singh PK, Singh S, Revankar SG, Chandrasekar PH, Kumar A. Evaluation of susceptibility and innate immune response in C57BL/6 and BALB/c mice during *Candida albicans* endophthalmitis. Invest Ophthalmol Vis Sci. 2020;61(11):31. [CrossRef]

19 Bleul T, Zhuang X, Hildebrand A, Lange C, Böhringer D, Schlunck G, et al. Different innate immune responses in BALB/c and C57BL/6 strains following corneal transplantation. J Innate Immun. 2021;13(1):49-59. [CrossRef]

20 Bergersen KV, Barnes A, Worth D, David C, Wilson EH. Targeted transcriptomic analysis of C57BL/6 and BALB/c mice during progressive chronic *Toxoplasma gondii* infection reveals changes in host and parasite gene expression relating to neuropathology and resolution. Front Cell Infect Microbiol. 2021;11:645778. [CrossRef]

21 Malm Tillgren S, Nieto-Fontarigo JJ, Cerps S, Ramu S, Menzel M, Mahmutovic Persson I, et al. C57Bl/6N mice have an attenuated lung inflammatory response to dsRNA compared to C57Bl/6J and BALB/c mice. J Inflamm (Lond). 2023;20(1):6. [CrossRef]

22 Krementsov DN, Case LK, Dienz O, Raza A, Fang Q, Ather JL, et al. Genetic variation in chromosome Y regulates susceptibility to influenza A virus infection. Proc Natl Acad Sci U S A. 2017;114(13):3491-6. [CrossRef]

23 Felgenhauer JL, Brune JE, Long ME, Manicone AM, Chang MY, Brabb TL, et al. Evaluation of nutritional gel supplementation in C57BL/6J mice infected with mouse-adapted influenza A/PR/8/34 virus. Comp Med. 2020;70(6):471-86. [CrossRef]

24 Honce R, Wohlgemuth N, Meliopoulos VA, Short KR, Schultz-Cherry S. Influenza in high-risk hosts-lessons learned from animal models. Cold Spring Harb Perspect Med. 2020;10(12):a038604. [CrossRef]

25 Avitsur R, Mays JW, Sheridan JF. Sex differences in the response to influenza virus infection: modulation by stress. Horm Behav. 2011;59(2):257-64. [CrossRef]

26 McGill J, Van Rooijen N, Legge KL. Protective influenza-specific CD8 T cell responses require interactions with dendritic cells in the lungs. J Exp Med. 2008;205(7):1635-46. [CrossRef]

27 Bot A, Bot S, Bona CA. Protective role of gamma interferon during the recall response to influenza virus. J Virol. 1998;72(8):6637-45. [CrossRef]

28 Brincks EL, Katewa A, Kucaba TA, Griffith TS, Legge KL. CD8 T cells utilize TRAIL to control influenza virus infection. J Immunol. 2008;181(7):4918-25. Erratum in: J Immunol. 2008;181(10)7428. [CrossRef]

29 Thomas PG, Dash P, Aldridge JR Jr, Ellebedy AH, Reynolds C, Funk AJ, et al. The intracellular sensor NLRP3 mediates key innate and healing responses to influenza A virus via the regulation of caspase-1. Immunity. 2009;30(4):566-75. [CrossRef]

30 Sun K, Metzger DW. Inhibition of pulmonary antibacterial defense by interferon-gamma during recovery from influenza infection. Nat Med. 2008;14(5):558-64. [CrossRef]

31 Wang X, Li M, Zheng H, Muster T, Palese P, Beg AA, et al. Influenza A virus NS1 protein prevents activation of NF-kappaB and induction of alpha/beta interferon. J Virol. 2000;74(24):11566-73. [CrossRef]

32 Robinson CM, Jung JY, Nau GJ. Interferon-γ, tumor necrosis factor, and interleukin-18 cooperate to control growth of *Mycobacterium tuberculosis* in human macrophages. Cytokine. 2012;60(1):233-41. [CrossRef]

33 Klein SL, Hodgson A, Robinson DP. Mechanisms of sex disparities in influenza pathogenesis. J Leukoc Biol. 2012;92(1):67-73. [CrossRef]

34 Huber SA, Sartini D. Roles of tumor necrosis factor alpha (TNF-alpha) and the p55 TNF receptor in CD1d induction and coxsackievirus B3-induced myocarditis. J Virol. 2005;79(5):2659-65. [CrossRef]